K selection in the decay of the (ν5/2[532]⊗3/2[411])4^{−} isomeric state in ^{102}Zr

F. Browne *et al.*

Phys. Rev. C **96**, 024309 — Published 15 August 2017

DOI: 10.1103/PhysRevC.96.024309

K-selection in the decay of the $(\nu\frac{5}{2}[532] \otimes \frac{3}{2}[411])4^-$ isomeric state in ^{102}Zr

F. Browne,[1,2,*] A. M. Bruce,[1] T. Sumikama,[3,2] I. Nishizuka,[3] S. Nishimura,[2] P. Doornenbal,[2] G. Lorusso,[2,4,5] P.-A. Söderström,[2] H. Watanabe,[2,6] R. Daido,[7] Z. Patel,[2,4] S. Rice,[2,4] L. Sinclair,[2,8] J. Wu,[2,9] Z. Y. Xu,[10,11] A. Yagi,[7] H. Baba,[2] N. Chiga,[3,2] R. Carroll,[4] F. Didierjean,[12] Y. Fang,[7] N. Fukuda,[2] G. Gey,[13,14] E. Ideguchi,[7] N. Inabe,[2] T. Isobe,[2] D. Kameda,[2] I. Kojouharov,[15] N. Kurz,[15] T. Kubo,[2] S. Lalkovski,[16] Z. Li,[9] R. Lozeva,[12,17] N. Nishibata,[7] A. Odahara,[7] Zs. Podolyák,[4] P. H. Regan,[4,5] O. J. Roberts,[1] H. Sakurai,[2] H. Schaffner,[15] G. S. Simpson,[13] H. Suzuki,[2] H. Takeda,[2] M. Tanaka,[7,18] J. Taprogge,[2,19,20] V. Werner,[21,22] and O. Wieland[23]

[1] *School of Computing, Engineering and Mathematics, University of Brighton, Brighton, BN2 4GJ, United Kingdom*
[2] *RIKEN Nishina Center, 2-1 Hirosawa, Wako-shi, Saitama 351-0198, Japan*
[3] *Department of Physics, Tohoku University, Aoba, Sendai, Miyagi 980-8578, Japan*
[4] *Department of Physics, University of Surrey, Guildford GU2 7XH, United Kingdom*
[5] *National Physical Laboratory, Teddington, Middlesex, TW11 0LW, United Kingdom*
[6] *IRCNPC, School of Physics and Nuclear Energy Engineering, Beihang University, Beijing 100191, China*
[7] *Department of Physics, Osaka University, Toyonaka, Osaka 560-0043, Japan*
[8] *Department of Physics, University of York, Heslington, York YO10 5DD, United Kingdom*
[9] *Department of Physics, Peking University, Beijing 100871, China*
[10] *Department of Physics, University of Tokyo, Hongo, Bunkyo-ku, Tokyo 113-0033, Japan*
[11] *Department of Physics, University of Hong Kong, Pokfulam Road, Hong Kong*
[12] *IPHC, CNRS/IN2P3, Université de Strasbourg, 67037 Strasbourg, France*
[13] *LPSC, Université Grenoble-Alpes, CNRS/IN2P3, F-38026 Grenoble Cedex, France*
[14] *ILL, 38042 Grenoble Cedex, France*
[15] *GSI Helmholtzzentrum für Schwerionenforschung GmbH, 64291 Darmstadt, Germany*
[16] *Department of Physics, University of Sofia, 1164 Sofia, Bulgaria*
[17] *CSNSM, CNRS/IN2P3, Université Paris-Sud, F-91405 Orsay Campus, France*
[18] *Research Center for Nuclear Physics (RCNP), Osaka University, Ibaraki, Osaka 567-0047, Japan*
[19] *Departamento de Física Teórica, Universidad Autónoma de Madrid, E-28049 Madrid, Spain*
[20] *Instituto de Estructura de la Materia, CSIC, E-28006 Madrid, Spain*
[21] *A. W. Wright Nuclear Structure Laboratory, Yale University, New Haven, Connecticut 06520, USA*
[22] *Institut für Kernphysik, Technische Universität Darmstadt, 64289 Darmstadt, Germany*
[23] *INFN Sezione di Milano, I-20133 Milano, Italy*

(Dated: Thursday 27th July, 2017)

The $(\nu\frac{5}{2}[532] \otimes \frac{3}{2}[411])$ 4^- state in ^{102}Zr, populated in the β-decay of ^{102}Y, has been measured to be isomeric with a mean lifetime of 9.5(7) ns. It decays via four transitions, two of which are $\Delta K = 2$ (to the 3^+ and 4^+ members of the 2^+_γ band) and one is $\Delta K = 4$ (to the 4^+ member of the ground state 0^+ band). The fourth (low-energy) transition is inferred to decay to an as-yet unassigned state. Hindrances of 10^6 were derived for the $\Delta K = 2$ transitions compared to Weisskopf estimates and the $\Delta K = 4$ transition hindered by a factor of 10^9. These values are consistent with the decay pattern of the analogous isomeric state in the neighbouring $N = 62$ nucleus ^{100}Sr and with the broader systematics of such transitions. A comparison of the hindrances for the $\Delta K = 4$ transitions suggests that ^{102}Zr is hardened against the γ degree of freedom compared to ^{100}Sr.

I. INTRODUCTION

In deformed nuclei, the K quantum number, which is the sum of the projection of the aligned angular momenta of nucleons, Ω, gives rise to a further electromagnetic transition selection rule [1], which states that the multipolarity of a transition, λ, must be less than, or equal to the change of K that it induces. Transitions that do not obey this relation are so-called "K-forbidden", and their degree of K forbiddeness is given by, $\nu = \Delta K - \lambda$. Isomeric levels which arise due to this rule are designated as "K-isomers".

Due, in part, to the availability of high-Ω orbitals near the Fermi-surface, the majority of measured K-isomers lie in the neutron-rich $A \approx 180$ region. Less abundant are K-isomers measured in the $A \approx 130$, 150 and actinide regions [2, 3]. Interestingly, the neutron-rich $A \sim 100$ region, where the K quantum number is expected to play a major role as a result of the prevalence of axially-deformed ground-states, has a scarcity of observed K isomers formed from multi-quasiparticle states, fewer than even the transuranic elements [3, 4]. Perhaps more intriguing is the formation of K-isomeric states in ^{98}Sr [5] and ^{100}Sr [6], without the anologous states in the respective zirconium isotones being observed as isomeric. Indeed, with the exception of ^{108}Zr [7, 8], no isomeric state, K, or otherwise, has been observed to date in the $A \geq 102$ zirconium isotopic chain. This was addressed in Ref. [9]

* frank@ribf.riken.jp

with arguments based on γ-softness of the potential energy surface (PES) of ^{104}Zr and the high energy of the 5^- candidate in ^{106}Zr. The lack of K-isomers in the higher-Z isotones could be attributed to a structural change from a rigid axially-symmetric deformation, to one susceptible to deformation in the γ degree of freedom.

The isotones ^{100}Sr and ^{102}Zr both have a two-quasi-neutron $K^\pi = 4^-$ state with the configuration, $\nu\frac{5}{2}[532] \otimes \frac{3}{2}[411]$ [6, 10]. In the case of ^{100}Sr, the 4^- state was found to be isomeric with mean lifetime $\tau = 123(10)$ ns [6]. Whilst ^{102}Zr has been studied using γ-ray spectroscopy following fission from a ^{248}Cf source [10], a ^{252}Cf source [11] and the β-decay of ^{102}Y [12, 13], none of the studies showed any evidence for the 1821-keV 4^- state with the same configuration in ^{102}Zr to be isomeric.

This work presents evidence for the isomerism of the 4^- state in ^{102}Zr using the high time- and energy-resolution spectroscopy of γ rays measured using a mixed array of high-purity germanium (HPGe) and cerium-doped lanthanum tri-bromide ($LaBr_3$(Ce)) detectors. The results are discussed in terms of the rigidity of the nucleus with respect to the γ degree of freedom.

II. EXPERIMENTAL DETAILS

The experimental investigation was carried out at the Radioactive Isotope Beam Factory, operated by the RIKEN Nishina Center and the Center for Nuclear Study, University of Tokyo. A $^{238}U^{86+}$ primary beam of average intensity 6.24×10^{10} particles/s was accelerated to an energy of 345 MeV/nucleon. The in-flight-abrasion-fission of the beam was induced by a 3-mm-thick ^{9}Be production target situated at the entrance of the Big RIKEN Projectile Fragment Separator (BigRIPS) [14]. The constituents of the secondary beam were selected and separated by the $B\rho$-ΔE-$B\rho$ method up until the 3rd focal plane of BigRIPS, thereafter, particle identification (PID) was performed using the TOF-$B\rho$-ΔE method [15]. The resultant PID plot is shown in Fig. 1, along with the software gates applied to select ions of ^{102}Y.

The secondary beam was implanted into the Wide-range Active Silicon Strip Stopper Array for β and Ion detection (WAS3ABi) [16], which detected ion implantations and their subsequent β-decay electrons. For this experiment, WAS3ABi comprised 5 layers of double-sided silicon-strip detectors (DSSSDs) detectors placed 0.5 mm apart, each with 60 vertical and 40 horizontal strips. The width and depth of each strip was 1 mm, giving a total active area of 60×40 mm^2. Correlation of ^{102}Y ions and their β decays was performed in an off-line procedure. The correlation condition was that a β decay event must have been detected within a 1.5 mm radius of an implanted ion, on the same DSSSD and have occurred within 1.5 s of the ion implantation. This time condition was chosen as it is $\sim$ 5 times the half-life of either

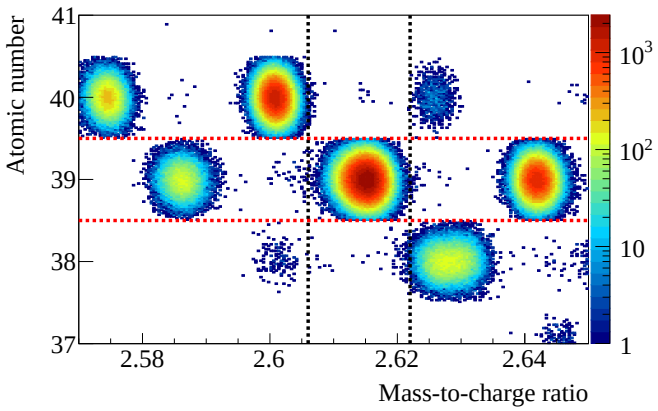

FIG. 1. (Color online) Particle identification plot of the secondary beam. The red and black dashed lines show the software gates applied to the atomic number and mass-to-charge ratio, respectively, to select ^{102}Y ions.

β-decaying states of ^{102}Y [12]. Plastic scintillators, hereafter referred to as "β-plastics", were placed up-stream and down-stream of WAS3ABi to measure, with high-time-precision, the occurrence of a β decay. The scintillators had dimensions of 45-mm height, 65-mm width and a depth of 2 mm.

High-resolution γ-ray spectroscopy of transitions de-exciting states populated through β decay was performed with the EUROBALL-RIKEN Cluster Array (EURICA) [17]. Each of its twelve cluster detectors comprised seven close-packed HPGe crystals which have a tapered hexagonal shape. An add-back procedure was employed such that γ rays which Compton scattered between crystals within a cluster had their energies summed. The fast-timing array comprised 18 $LaBr_3$(Ce) detectors [18, 19], each of 38.1 mm diameter and 50.8 mm length. The timing properties of the $LaBr_3$(Ce) detectors mean that the γ-ray times can be measured with a precision of $\sim$2 orders of magnitude greater than in the HPGe detectors of EURICA. The efficiency of EURICA and $LaBr_3$(Ce) array at 1.3 MeV was measured to be $\sim$10% and $\sim$1%, respectively.

III. RESULTS

In order to identify γ-ray decay from any isomeric states in ^{102}Zr, separate energy-time matrices were constructed for EURICA and the fast-timing $LaBr_3$(Ce) array. In both cases the time difference was measured between the detection of a γ ray in the respective detector and the β electron of ^{102}Y. This latter was obtained from the average of the left and right photo-multiplier tube signals of the upstream β plastic. Only the upstream plastic was considered since implantations occurred solely in the first layer of WAS3ABi, resulting in a negligible β electron detection efficiency in the downstream β plastic.

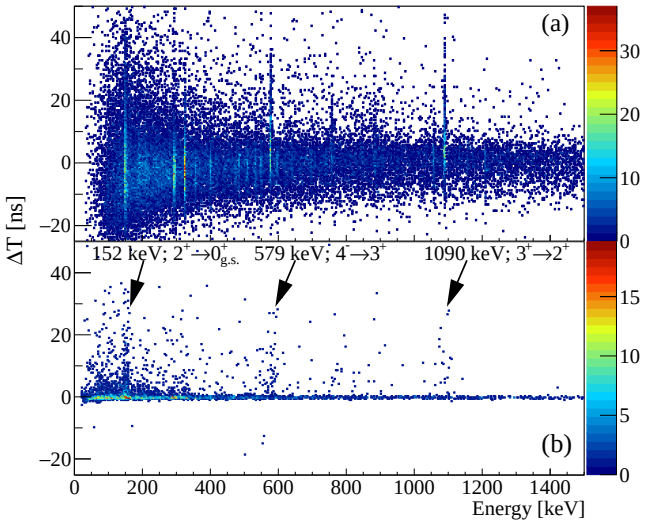

FIG. 2. (Color online) Energy-time matrices measured in coincidence with a position-correlated β decay occurring within 1.5 s of an ^{102}Y ion implantation in (a) EURICA and (b) the $LaBr_3$(Ce) array. The transitions that are delayed due to the isomerism of the 4^- state are labelled in the $LaBr_3$(Ce) matrix and are also evident in the EURICA matrix.

The resultant matrices measured in EURICA and the $LaBr_3$(Ce) array are shown in Figs. 2(a) and 2(b), respectively. Both matrices show clear delayed structures, as expected for transitions originating from an isomeric state, corresponding to the 579- and 1090-keV transitions in ^{102}Zr, which are known [11, 12] to form a cascade that de-excite the two-quasi-neutron 1821-keV 4^- state. Additionally, the 152-keV, $2_1^+ \rightarrow 0_{g.s}^+$ transition is visible in the delayed portion of the $LaBr_3$(Ce) matrix. It should be noted that despite employing a similar experimental set-up, the isomerism apparent in Fig. 2 was not reported in Ref. [13], this is due to the superior time resolution of the β-plastics over DSSSDs. Moreover, it is evident that the superior time resolution of the $LaBr_3$(Ce) array compared to EURICA means that the proportion of the delayed structure outside of the prompt region is greater in Fig. 2(b) than in 2(a).

A. EURICA HPGe array

Figure 3 shows a γ-ray energy spectrum measured in EURICA in prompt coincidence with an ^{102}Y-correlated β-decay measured in WAS3ABi, with no condition that the decay should be measured also in the β-plastics. By neglecting the β-plastics, which for this experiment had an efficiency of ∼50%, statistics in the γ-ray spectrum were approximately doubled.

The level scheme associated with the decay of the 1821-keV 4^- state in ^{102}Zr measured in this work is shown in Fig. 4 and is consistent with those in Refs. [10–13]. However, a discrepancy between the branching ratios

TABLE I. The intensities of γ-ray transitions that de-excite the isomeric 4^- state of ^{102}Zr, normalized to the 579-keV transition

E_γ [keV]	I_γ This work	Ref. [11]
(27)	[6(1)][a]	-
	[4(1)][b]	-
283	7(1)	76(4)
579	100(4)	100(5)
1343	3(1)	6(2)

[a] I_γ calculated from total transition intensity, assuming $E1$ decay (see text for details).
[b] Assuming $M1$ decay (see text for details).

of the transitions that de-excite the 4^- state is observed between this work and Ref. [11]. The details are listed in Tab. I. In Ref. [11] the intensity of the 283-keV transition was measured to be similar to that of the 579-keV transition. The spectrum shown in Fig. 3(a) shows a much weaker 283-keV transition and this observation is corroborated by the spectrum obtained from a prompt coincidence with the 160-keV transition which is shown in Fig. 3(b). The data in Ref. [11] were obtained from a ^{252}Cf fission source and this discrepancy could be attributed to the contamination of the 283-keV peak in Ref. [11] by the 283.4-keV transition in ^{147}Ce, which is a fission partner to ^{102}Zr. The total intensity of the inferred 27-keV transition has been obtained from the sum of the intensities of the 551- and 757-keV transitions in the 160-keV gate and the corresponding γ-ray intensities quoted in Tab. I calculated for both $E1$ ($\alpha = 4.63(8)$ [20]) and $M1$ ($\alpha = 8.62(16)$ [20]) transitions. An alternative transition of ∼ 187 keV from the 1981-keV 5^- state to the 1793-keV (3,4) state can be excluded from its non-observation in singles and coincidence spectra. The 283- and 1343-keV transitions are very weak in the 160-keV gated spectrum and their relative intensities have therefore been obtained from the singles spectrum shown in Fig. 3(a). It is evident from Fig. 3(c) that there is a prominent background peak adjacent to the 1343-keV peak of interest. This was found to be the 1346-keV transition originating from the β decay of ^{103}Zr, the parent of which (^{103}Y) is seen to be a major component of the cocktail beam, shown in Fig. 1. A two-Gaussian fit with a constant background was performed, the widths of the peaks were fixed according to standard-source calibration measurements and the centroids constrained to $\pm 1\sigma$ of their adopted values [21, 22].

To exclude the possibility that the retarded decay of the 4^- state results from an isomeric 5^- state, the β-γ time-difference (ΔT) of the $5^- \rightarrow 4^-$ 160-keV transition was taken. This is shown in Fig. 5 along with its background, and shows no clear delayed structure. Figure 6 shows the sum of the time-difference projections of the 579- and 1090-keV transitions of the EURICA matrix shown in Fig. 2(a). Also shown, are the prompt

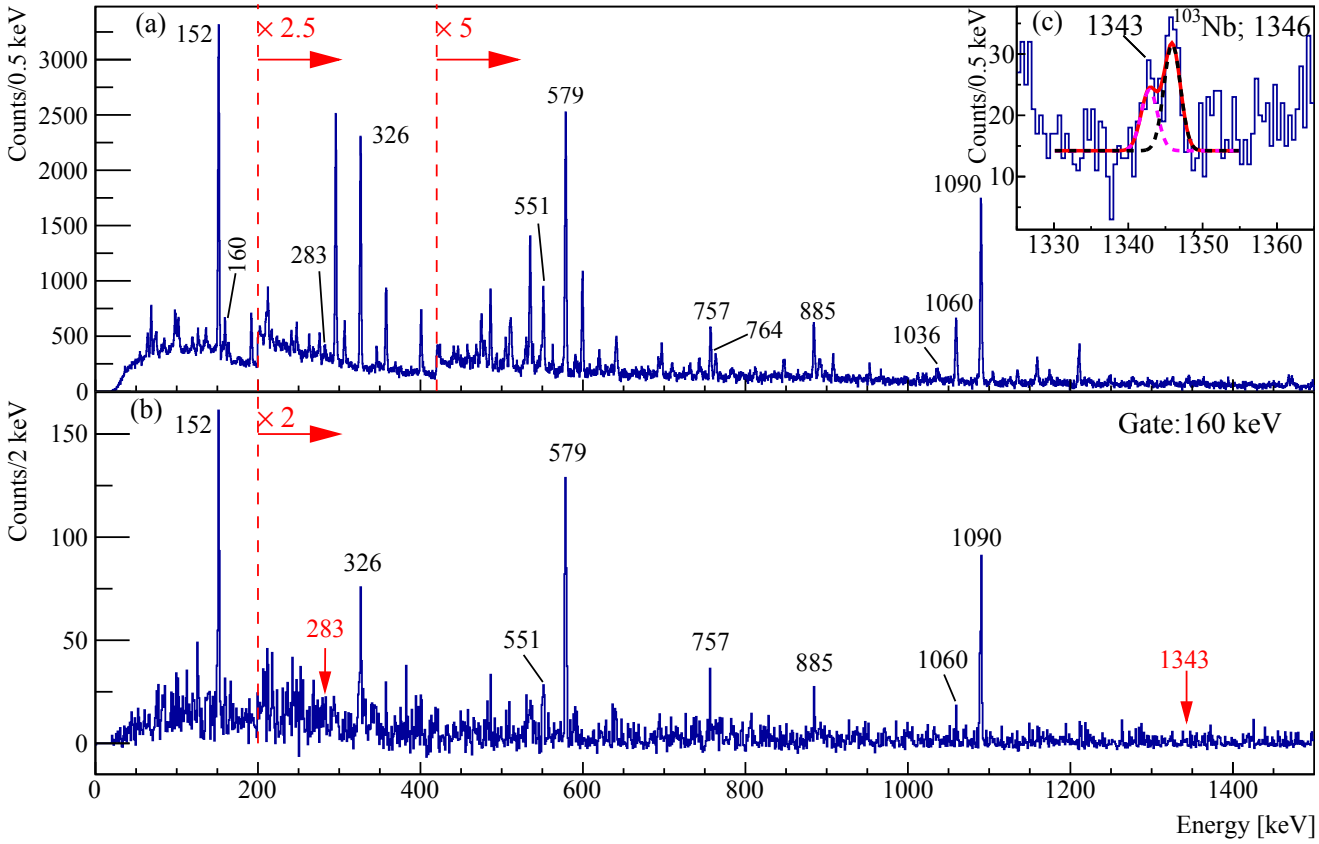

FIG. 3. (Color online) The γ-ray energy spectrum measured by EURICA in coincidence with a position-correlated β-decay occurring within 1.5 s of an implanted ^{102}Y ion. The labeled energies are those that correspond to transitions that are in the decay cascade originating from the 4^- isomeric state. The other energy peaks are due to the decay of levels populated in the β-decay of ^{102}Y which are independent of the cascade from the 4^- state and the random correlations of β-decays to nuclei other than ^{102}Y. The magnification factors shown in red are always given with respect to the original spectrum. (b) The spectrum measured in prompt ($\Delta T < 200$ ns) coincidence with the 160-keV transition. The red labels in (b) indicate the positions of the 283- and 1343-keV transitions. (c) Is an expanded view of the region around the 1343-keV transition showing the result of a double-Gauss fit on a constant background, see text for details.

spectra for the neighboring background regions, which serve as the backgrounds for the time projections of the transitions. It is apparent that after 10 ns, the background becomes negligible for both energies. The shape of the decay curve is consistent with the decay of only one isomeric state. The single-component exponential fit between the values of 10 and 35 ns yields a result of 9.6(8) ns for the mean lifetime of the 4^- state.

B. $LaBr_3$(Ce) array

The prompt and delayed energy projections of the $LaBr_3$(Ce) energy-time matrix shown in Fig. 2(b) are shown in Fig. 7(a). In the delayed projection, the 152- and 579-keV transitions are prominent, and the 1090-keV transition and its Compton continuum are evident. Meanwhile, in the prompt spectrum the dominant peaks belong to the $2_1^+ \rightarrow 0_{g.s}^+$ and $4_1^+ \rightarrow 2_1^+$ transitions, at 152- and 326-keV, respectively. Time projections of the sum of the full-energy peaks of the 579- and 1090-keV transitions are shown in Fig. 7(b). A single-exponential fit was applied between 0.5 and 35 ns yielding a mean lifetime of 9.4(14) ns, consistent with the EURICA result.

IV. DISCUSSION

The weighted average of the mean lifetimes measured with the the two different detector types is $\tau = 9.5(7)$ ns. The fact that there are two long-lived states in ^{102}Y which β decay directly into ^{102}Zr [12] does not affect the measurement of the 4^- level lifetime made here since the two cascading transitions, 579 and 1090 keV, that are used originate only from feeding from the high-spin β-decaying state in ^{102}Y.

The decay details of the 4^- state in ^{102}Zr are given in Tab. II along with details of the decay of the analogous state in ^{100}Sr. In the case of ^{100}Sr, the levels at 1414 and 1501 keV, populated by the 204- and 118-keV transitions, respectively, have been observed in the β decay of ^{100}Rb [23] and tentatively assigned as $J^\pi = (3, 4^+)$. In the subsequent discussion, they are assumed, based on analogy with ^{102}Zr, to be the 3^+ and 4^+ members of the γ band, respectively. Column 7 of Tab. II lists the Weisskopf hindrance factors, defined as the ratio of the partial lifetime to the single-particle estimate, $F_W = \tau^\gamma/\tau^{W.e.}$. For all transitions except that with energy 27 keV in ^{102}Zr, an $E1$ multipolarity has been assumed. In the case of the 27-keV transition, both $E1$ and $M1$ possible multipolarities are calculated since the parity of the 1793-keV level, which it populates, is unknown. Of the eight transitions listed in Tab. II, only that of energy 579 keV has been measured as a pure dipole character [11].

A recent compilation of the decay properties of multi-quasiparticle K isomers [2] has provided a description of the systematic behavior of $\log(F_W)$ as a function of ΔK. The data for $E1$ transitions are shown in black in Fig. 8(a) and for $M1$ in Fig. 8(b). The red stars indicate the values for the transitions in ^{102}Zr measured in this work. The values for the two $\Delta K = 2$ and one $\Delta K = 4$ transitions are consistent with the $E1$ systematics. For the 27-keV transition, the data is consistent with a $\Delta K = 1$ dipole transition of either multipolarity and is, therefore, unable to fix the nature of the transition, or the parity of the 1793-keV level.

The energy of the 2^+_γ state is an indicator of the triaxiality that a nucleus exhibits. When it is lower, the nucleus is more soft to vibrational motion, or static deformation in the axially asymmetric γ-degree of freedom. It has been observed [25] that the hindrance of $E2$ transitions de-populating K-isomeric states is positively correlated with the energy of the bandhead of the quasi-γ band. This is an experimental demonstration that a nucleus which is more susceptible to triaxial deformation will also be more prone to K-mixing. This observation is not limited to $E2$ decays. In order to better quantify the magnitude of K-mixing, it is useful to measure the "hindrance per degree of K-forbiddenness" which is given in the last column of Tab. II for the two $\Delta K = 4$ transitions. This is defined as,

$$f_\nu = F_W^{1/\nu}, \tag{1}$$

where ν is the degree of K-forbiddenness, given by $\nu = \Delta K - \lambda$, where λ is the multipolarity of the transition. The f_ν of the $4^-_{K^\pi=4^-}$ to $4^+_{K^\pi=0^+}$ transition is larger in ^{102}Zr (1351) than in ^{100}Sr (808). These nuclei have similar 2^+_1 energies (152 keV for ^{102}Zr and 129 keV for ^{100}Sr) and E(4^+_1)/E(2^+_1) values (3.145 for ^{102}Zr and 3.240 for ^{100}Sr), suggesting their deformation will be similar. However, the relative position of the bandhead of the γ-band of ^{100}Sr (E_γ =1257 keV, $R_{2_\gamma/2_1^+} = 9.7$) compared to the same state in ^{102}Zr (E_γ =1036 keV, $R_{2_\gamma/2_1^+} = 6.8$), would suggest that the latter is more susceptible to somewhat triaxial features. As such, the decay of states in

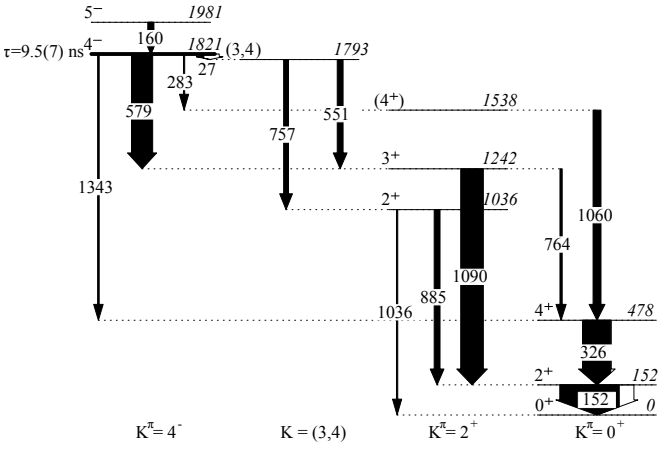

FIG. 4. The partial level scheme of ^{102}Zr observed in this work from the β-decay of ^{102}Y. It displays only transitions which feed, or are fed by the isomeric 4^- state. The widths of the arrows indicate the relative intensity of each transition. The level and transition energies are given in keV. The J^π assignments are taken from Ref. [11].

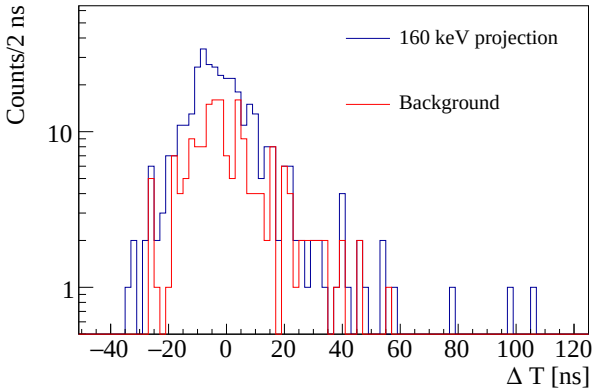

FIG. 5. (Color online) The time-difference projection of the 160-keV transition relative to the β-decay time (blue) and its background (red), using the EURICA HPGe detectors, taken from Fig 2(a). No delayed component, or shift of centroid is visible, as it is with Fig. 6.

^{102}Zr would be expected to be less hindered by the K-selection rule than in ^{100}Sr [25]. This is contrary to the observation. In the current work, it is unknown if the small energy difference of the quasi-γ band is sufficient to make an appreciable effect on the K-mixing between the two nuclei, or if there is some other overriding structural effect that is responsible for the enhancement of the adherence to the K selection rule in ^{102}Zr.

The F_W value listed in Tab. II shows that for the $4^-_{K^\pi=4^-} \rightarrow 3^+_\gamma$ transition in ^{100}Sr is an order of magnitude higher than in ^{102}Zr. Within the context of this work, this result is difficult to understand and requires further experimental investigation. It is possible that the $J^\pi = 3^+_\gamma$ assumption of the state in ^{100}Sr, or ^{102}Zr was erroneous, or that, as with the 283-keV reported in this work, the literature value of the intensity of the 204-keV transition in ^{100}Sr is incorrectly reported. Whilst the F_W values of the 58- and 27-keV transitions in ^{100}Sr and ^{102}Zr, respectively, are also inconsistent, the lack of information regarding their nature inhibits meaningful discussion in this work.

It is worth noting that despite ^{102}Zr having a larger f_ν value than ^{100}Sr for the $4^- \rightarrow 4^+_{g.s.}$ transition, the lifetime is shorter by an order of magnitude. This is due to the difference of the energies of the transitions feeding the 4^+_γ and 3^+_γ states from the 4^- state.

V. CONCLUDING REMARKS

In summary, we have provided the first measurement of the lifetime of the 1821-keV isomeric state in ^{102}Zr which decays with a mean lifetime of 9.5(7) ns to three different structures. The hindrances of the de-exciting γ-ray transitions are mostly consistent with those from the known K-isomer in the isotone ^{100}Sr and support the conclusion of the level being a $(\nu\frac{5}{2}[532] \otimes \frac{3}{2}[411])$ $K^\pi = 4^-$ isomer. This measurement provides a valuable data point in understanding the role K isomerism plays in a mass region where there is a scarcity of information of multi-quasiparticle K-isomeric states. Compared to the analogous transitions in ^{100}Sr, a 60% increase in f_ν was observed for the $E1$ decay to the ground-state band, the F_W for the decay to the 4^+_γ state was observed to be consistent and the F_W for the decay to the 3^+_γ state reduced by an order of magnitude. Further investigation into the lifetimes and decays of the analogous states in ^{98}Kr and ^{104}Mo is required in order to obtain a more conclusive understanding of this feature.

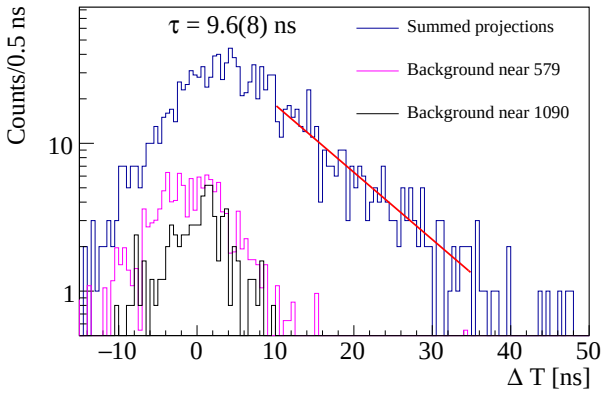

FIG. 6. (Color online) The summed time-difference projections of the 579- and 1090-keV transitions (blue) relative tot he β-decay time, using the EURICA HPGe detectors, taken from Fig 2(a). The background measurements, taken as an average of a representative region either side of the signal regions, are shown as dashed and solid black lines, respectively. The red line is a single-component exponential fit.

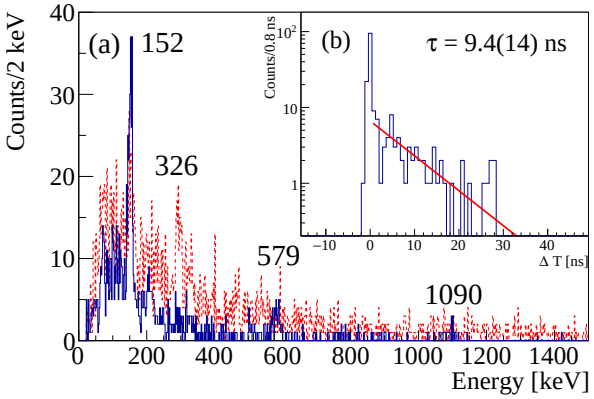

FIG. 7. (Color online) (a) The prompt ($\Delta T < \pm 0.5$ ns, red) and delayed ($0.5 < \Delta T < 50$ ns, blue) energy projection of the $LaBr_3$(Ce) energy-time matrix shown in Fig. 2(b). (b) The sum of the time-difference projections of the 579- and 1090-keV transitions, taken from Fig. 2(b). The red line is a single-component exponential fit.

ACKNOWLEDGMENTS

This work was supported by JSPS KAKENHI Grant Nos. 26800117 and 25247045. UK authors were supported by STFC Grant Nos. ST/J000132/1, ST/J000051/1 and ST/K502431/1. P.H.R. acknowledges support from the UK National Measurement Office. P.-A.S. was financed by JSPS Grant No. 23 01752 and the RIKEN Foreign Postdoctoral Researcher Program. V.W. was supported by DOE Grant No. DE-FG02-91ER-40609 and the German BMBF Grant No. 05P12RDFN8. J.T. was financed by Spanish Ministerio de Ciencia e Innovación under Contract Nos. FPA2009-13377-C02 and FPA2011-29854-C04. F. B. is grateful for helpful discussions with Prof. P. M. Walker. We acknowledge the EUROBALL Owners Committee for the loan of germanium detectors and the PreSpec Collaboration for the readout electronics of the cluster detectors

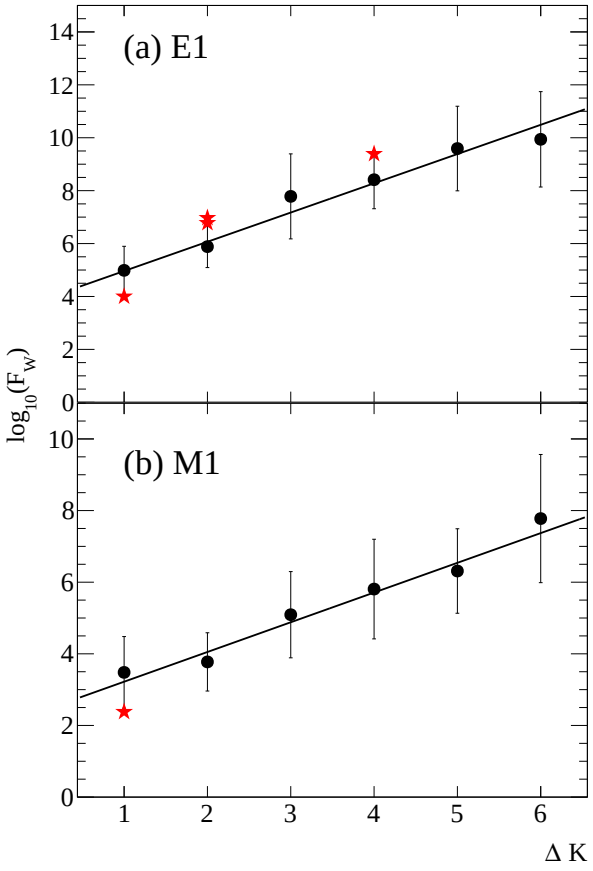

FIG. 8. (a) Hindrance factors, $\log F_W$, of $E1$ transitions as a function of ΔK. The black points and line show the systematic behaviour of the experimentally confirmed hindrances [2]. The red stars represent the logarithm of hindrances measured in ^{102}Zr for which the uncertainties are smaller than the data points. (b) The same as (a) for $M1$ transitions.

[1] M. Goldhaber and A. W. Sunyar, *in α-, β- and γ-ray Spectroscopy* (North Holland, Amsterdam, 1965) p. 945.
[2] F. Kondev, G. Dracoulis, and T. Kibédi, At. Data. Nucl. Data Tables **103-104**, 50 (2015).
[3] P. M. Walker, AIP Conf. Proc. **819**, 16 (2006).
[4] P. M. Walker and F. R. Xu, Phys. Scr. **91**, 013010 (2016).
[5] G. Lhersonneau, B. Pfeiffer, R. Capote, J. M. Quesada, H. Gabelmann, and K.-L. Kratz, Phys. Rev. C **65**, 024318 (2002).
[6] B. Pfeiffer, G. Lhersonneau, H. Gabelmann, and K. L. Kratz, Z. Phys. A **353**, 1 (1995).
[7] T. Sumikama *et al.*, Phys. Rev. Lett. **106**, 202501 (2011).
[8] D. Kameda *et al.*, Phys. Rev. C **86**, 054319 (2012).
[9] Y. Shi, P. M. Walker, and F. R. Xu, Phys. Rev. C **85**, 027307 (2012).
[10] J. L. Durell *et al.*, Phys. Rev. C **52**, R2306 (1995).
[11] K. Li *et al.*, Phys. Rev. C **78**, 044317 (2008).
[12] J. C. Hill, D. D. Schwellenbach, F. K. Wohn, J. A. Winger, R. L. Gill, H. Ohm, and K. Sistemich, Phys. Rev. C **43**, 2591 (1991).
[13] A. M. Bruce *et al.*, J. Phys.: Conf. Ser. **381**, 012053 (2012).
[14] T. Kubo *et al.*, Prog. Theor. Exp. Phys. **2012**, 03C003 (2012).
[15] N. Fukuda, T. Kubo, T. Ohnishi, N. Inabe, H. Takeda, D. Kameda, and H. Suzuki, Nucl. Instrum. Methods B **317**, 323 (2013).
[16] S. Nishimura, Prog. Theor. Exp. Phys. **2012**, 03C006 (2012).
[17] P.-A. Söderström *et al.*, Nucl. Instrum. Methods B **317, Part B**, 649 (2013).
[18] O. J. Roberts, A. M. Bruce, P. H. Regan, Z. Podolyák, C. M. Townsley, J. F. Smith, K. F. Mulholland, and A. Smith, Nucl. Instrum. Methods A **748**, 91 (2014).
[19] Z. Patel *et al.*, RIKEN Accel. Prog. Rep. **47**, 13 (2014).
[20] T. Kibédi, T. Burrows, M. Trzhaskovskaya, P. Davidson, and C. N. Jr., Nucl. Instrum. Methods Phys. Res., Sect. A **589**, 202 (2008).

[21] D. D. Frenne, Nucl. Data Sheets **110**, 1745 (2009).
[22] D. D. Frenne, Nuclear Data Sheets **110**, 2081 (2009).
[23] G. Lhersonneau, B. Pfeiffer, H. Gabelmann, and K.-L. Kratz (The ISOLDE Collaboration), Phys. Rev. C **63**, 054302 (2001).
[24] B. Singh, Nucl. Data Sheets **109**, 297 (2008).
[25] T. R. Saitoh, N. Saitoh-Hashimoto, G. Sletten, R. A. Bark, G. B. Hagemann, and B. Herskind, Phys. Scr. **2000**, 67 (2000).

TABLE II. The details of the decay of the 4^- states in ^{100}Sr and ^{102}Zr.

Nucleus	τ [ns]	E_γ [keV]	σL[a]	I_γ	α[b]	F_W[c]	ΔK	f_ν
^{100}Sr[d]	123(10)[6]	58	$(E1)$	0.95(24)	0.4928	$6.34(204) \times 10^6$		
$E_{4^-} = 1618$ keV		118	$(E1)$	5.2(10)	0.06239	$9.60(23) \times 10^6$	2	
		204	$(E1)$	5.2(10)	0.01254	$4.99(12) \times 10^7$	2	
		1202	$(E1)$	100(14)	0.0002218	$5.27(128) \times 10^8$	4	808
^{102}Zr	9.5(7)	27.2(5)	$(E1)$	[6(1)]	4.63	$1.0(2) \times 10^4$		
$E_{4^-} = 1821$ keV			$(M1)$	[4(1)]	8.62	241(48)		
		282.6(3)	$(E1)$	7(1)	0.00573	$9.31(155) \times 10^6$	2	
		578.9(3)	$E1$	100(4)	0.000916	$5.98(56) \times 10^6$	2	
		1343(1)	$(E1)$	3(1)	0.000303	$2.47(71) \times 10^9$	4	1351

[a] All transitions have assumed multipolarities except for 579 keV for which $E1$ has been measured [11].
[b] Conversion coefficients summed over all electron shells [20].
[c] Weisskopf hindrance factor defined as the ratio of the partial mean lifetime τ^γ to the Weisskopf estimate $\tau^{W.e.}$.
[d] Intensities taken from Ref. [24].